Accepted Manuscript

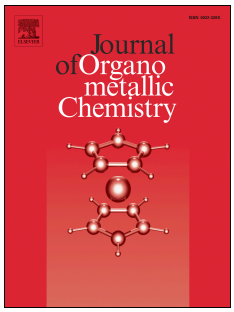

Synthesis and characterization of piano-stool ruthenium complexes with N, N′-pyridine imine bidentate ligands and their application in styrene oxidation

Joel M. Gichumbi, Holger B. Friedrich, Bernard Omondi

PII: S0022-328X(16)30048-1

DOI: 10.1016/j.jorganchem.2016.02.015

Reference: JOM 19399

To appear in: *Journal of Organometallic Chemistry*

Received Date: 28 October 2015

Revised Date: 5 February 2016

Accepted Date: 11 February 2016

Please cite this article as: J.M. Gichumbi, H.B. Friedrich, B. Omondi, Synthesis and characterization of piano-stool ruthenium complexes with N, N′-pyridine imine bidentate ligands and their application in styrene oxidation, *Journal of Organometallic Chemistry* (2016), doi: 10.1016/j.jorganchem.2016.02.015.

Graphical Abstract

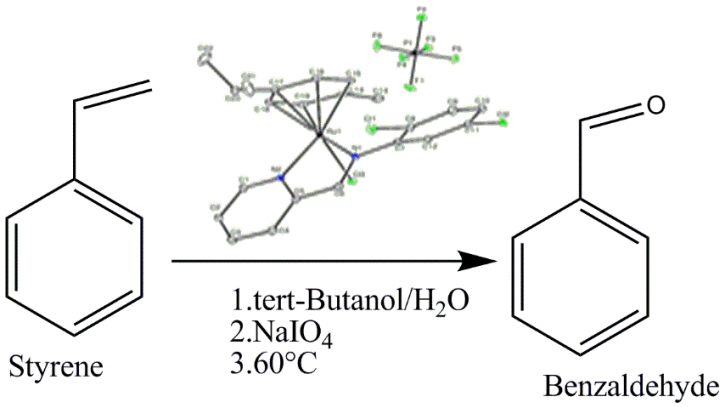

Synthesis and characterization of piano-stool ruthenium complexes with N, N′-pyridine imine bidentate ligands and their application in styrene oxidation.

Joel M. Gichumbi, Holger B. Friedrich*, Bernard Omondi.

* School of Chemistry, University of KwaZulu-Natal, Private Bag X54001, Durban 4001, South Africa.

*Corresponding author. Tel.: +27 312603107; fax: +27 312603091. E-mail address: friedric@ukzn.ac.za (H.B. Friedrich).

Abstract

The new complexes [(η^6-arene)RuCl(C_5H_4N-2-CH=N-R)]PF_6 (arene = C_6H_6 with R = 4-flourophenyl (**1**), 4-chlorophenyl (**2**), 4-bromophenyl (**3**), 4 -iodophenyl (**4**), 2, 5-dichlorophenyl (**5**) or *p*-cymene with R = 4-flourophenyl (**6**), 4-chlorophenyl (**7**), 4-bromophenyl (**8**), 4-iodophenyl (**9**), 2, 5 - dichlorophenyl (**10**)) have been synthesized by reacting the ruthenium arene precursors [(η^6-arene)Ru(μ-Cl)Cl]$_2$, with the N, N′-bidentate ligands in a 1:2 ratio. Full characterization of all complexes was accomplished using ^{1}H and ^{13}C NMR, elemental analyses, UV-Vis spectroscopy, thermal analysis, IR spectroscopy and single crystal x-ray structures for compounds **7** and **10**. The single crystal structures confirmed coordination of the ligand to the ruthenium(II) centre. The Ru(II) center has a pseudo-octahedral three legged piano stool geometry in which the arene ring occupies the apex of the stool and the ruthenium is coordinated to the N, N'-bidentate ligand and a chloride ligand at the base of the stool. Two polymorphs of **7** were identified. The synthesized Ru(II) complexes were tested as catalysts for the oxidation of styrene to benzaldehyde using $NaIO_4$ as a co-oxidant. All complexes were active catalysts for styrene oxidation and they gave high yields of benzaldehyde as the major product.

Key words: Ruthenium arene, N, N-bidentate ligands, styrene oxidation, benzaldehyde, mechanism

1. Introduction

The oxidation of olefins is an important reaction to fragment large compounds and to introduce the oxygen functionality into their backbone. This transformation has played an extensive and important role in the production of fine and pharmaceutical grade chemicals [1]. Traditionally, ozonolysis has been used as a general technique to obtain aldehydes or carboxylic acids. However, major safety concerns and inconvenience associated with ozone generation has prompted researchers to develop catalytic metal-based systems for application in olefin oxidation [2].

Amongst the metals that have potential application in catalytic selective oxidation, ruthenium takes a special position owing to its versatility [3]. The utilization of ruthenium in olefin

oxidation has been investigated widely [4]. However, there are very few reports on the use of half-sandwich ruthenium complexes containing nitrogen ligands in olefin oxidation [5]. The half-sandwich arene ruthenium(II) complexes with nitrogen-donor ligands have received a lot of attention from researchers due to their potential applications in photochemical devices [6], catalysis [7-13] and applications as cytotoxic agents for anticancer therapy [14-20]. This versatility of arene ruthenium(II) complexes in catalysis may be attributed to the existence of three labile coordinative sites and a rigid arene ring occupying the other three coordinate sites [21].

The nitrogenous donor ligands are very attractive when coordinated to ruthenium complexes because the steric and electronic properties around the metal centre can be easily changed with these ligands [22]. One type of nitrogen-donor ligand is the bidentate pyridine-imine Schiff base. The reactions of some pyridine-imine Schiff bases with ruthenium have been reported [23-25]. These complexes exhibited good activities as cytotoxic agents in human cancer cell lines and in aqueous phase hydroformylation [8,26].

To the best of our knowledge, no research on the influence of altering the arene ring on the styrene oxidation reaction has been undertaken. This prompted us to investigate the reactivity of $[(\eta^6\text{-arene})Ru(\mu\text{-}Cl)Cl]_2$ [arene = C_6H_6 or *p*-cymene] with pyridine-imines with electron withdrawing halogen atoms as substituents in the *para*-position. The formation of $[(\eta^6\text{-arene})RuCl(C_5H_4N\text{-}2\text{-}CH{=}N\text{-}R)]PF_6$ complexes (where R = 4-flourophenyl, 4-chlorophenyl, 4-bromophenyl, 4-iodophenyl, 2, 5-dichlorophenyl and arene = C_6H_6, *p*-cymene) are reported. All the new compounds were fully characterized by various analytical techniques and the structures of two complexes have been confirmed using single crystal x-ray crystallography. These complexes have been employed in styrene oxidation using $NaIO_4$ as the oxidant and excellent conversions and yields towards benzaldehyde were achieved. In addition, steric and electronic effects on the catalytic activity and selectivity of the complexes in the styrene oxidation reactions were explored.

2. Experimental

All manipulations were carried out under an inert atmosphere (UHP nitrogen) using Schlenk techniques. Analytical grade acetonitrile (Merck) was dried over phosphorous (V) oxide, reagent grade diethyl ether (Merck) was distilled from sodium/benzophenone and stored over molecular sieves and ethanol was dried over Mg/I_2. The chemical reagents: 1, 4-cyclohexadiene, α-phellandrene, 2-pyridinecarboxaldehyde, 4-chloroaniline, 4-flouroaniline, 4-bromoaniline, 4-iodoaniline and 2, 5-dichloroaniline were purchased from Sigma-Aldrich and utilized as received. Melting points were measured on an Ernest Leitz Wetzlar hot stage microscope. Elemental analyses were performed on Thermal-Scientific Flash 2000 CHNS/O analyzer. Infrared spectra were recorded using an ATR Perkin Elmer Spectrum 100 spectrophotometer between 4000-400 cm^{-1} in the solid state. Mass spectra were recorded via a Waters Micromass LCT Premier TOF-MS analyzer by direct infusion and ESI in the positive mode. Acetonitrile

(100%) was used as a mobile phase and 10 μL of the sample injected at 0.3 ml/min flow rate. Thermogravimetric analysis (TGA) was performed on a SDTQ600 TGA-DSC in a nitrogen atmosphere. ^{1}H and ^{13}C NMR spectra were recorded on Brucker Top Spin 400 and 600 MHz spectrometers using deuterated DMSO-d_6 from Sigma-Aldrich. The precursors of [(η^6-arene)Ru(μ-Cl)Cl]$_2$, where arene = C_6H_6 or *p*-cymene, were prepared following reported methods [27]. The pyridine-imine ligands were synthesized according to reported procedures [28].

2.1 General procedure for the synthesis of [(η^6-arene)RuCl(C_5H_4N-2-CH=N-R)]PF_6 , 1-5

The complexes were prepared using a modified method from Gomez *et al*. [29]. The precursor complex [(η^6-arene)Ru(μ-Cl)Cl]$_2$ (0.20 mmol) was dissolved in acetonitrile (10 ml) and added to the ligands **a-e** (C_5H_4N-2-CH=N-R]PF_6 (R = 4-flourophenyl (**a**), 4-chlorophenyl (**b**), 4-bromophenyl (**c**), 4-iodophenyl (**d**), 2,5-dichlorophenyl (**e**)), in slight excess (0.43 mmol), dissolved in acetonitrile. The mixture was stirred for 3 h and the solvent evaporated giving a yellow oil that was then treated with NH_4PF_6 (0.43 mmol) in 10 ml ethanol. The mixture was stirred in an ice bath maintained at zero degrees for two hours resulting in orange or yellow solids, which were isolated by gravity filtration, washed with diethyl ether and dried *in vacuo*. The yields and characterization data for each salt are given below.

1 $[C_{18}H_{15}ClN_2F_1Ru]PF_6$

Orange powder. Yield 70%. m.p. 210.2 °C $_{(decomp.).}$ ^{1}H NMR (600 MHz, DMSO-d_6): δ 9.66 (d, J_{HH} = 5.22 Hz, 1H, H^1), δ 8.90 (s, 1H, CH=N, H^6), δ 8.30 (d, J_{HH} = 5.0 Hz, 2H, H^2 , H^4), δ 8.26 (m, 3H, H^3, H^8, H^{12}), δ 7.88 (m, 2H, H^9, H^{11}), δ 5.96 (s, 6H, C_6H_6). ^{13}C NMR (400 MHz, DMSO- d_6): δ 168.83 (C^6); δ 161.92 (C^1); δ 156.84 (C^5); δ 155.11 (C^4); δ 148.72 (C^3); δ 140.61 (C^2); δ 130.54 (C^7); δ 129.33 (C^8, C^{12}); δ 125.25 (C^9); δ 116.93 (C^{11}); δ 87.87 (C_6H_6). IR (KBr, cm^{-1}): 1615.6 ν (C=N), 824.5 ν(P-F). Anal. Calcd. for $[C_{18}H_{15}ClN_2F_1Ru]PF_6$ C, 38.62; H, 2.70; N, 5.00. Found: C, 38.70; H, 2.64; N 4.85. MS (ESI, M/Z): 414.9950 $[C_{18}H_{15}ClN_2F_1Ru]^+$

2 $[C_{18}H_{15}Cl_2N_2Ru]PF_6$

Yellow powder, Yield 74%. m.p. 204.2 °C $_{(decomp.)}$. ^{1}H NMR (600 MHz, DMSO- d_6): δ 9.67 (d, J_{HH} = 5.40 Hz, 1H, H^1), δ 8.92 (s, 1H, H^6), δ 8.34 (m, 2H, H^2 , H^4), δ 7.90 (m, J_{HH} = 5.22 Hz, 1H, H^3), δ 7.84 (t, 2H, H^8, H^{12}), δ 7.72 (t, J_{HHH} = 5.84 Hz, 2H, H^9, H^{11}), δ 5.97 (s, 6H, C_6H_6). ^{13}C NMR (400 MHz, DMSO- d_6): δ 169.09 (C^6); δ 156.80 (C^1); δ 155.0 (C^5); δ 150.9 (C^4); δ 140.60 (C^3); δ 134.5 (C^2); δ 130.7 (C^7); δ 129.99 (C^8, C^{12}); δ 129.39 (C^9); δ 124.81 (C^{11}); δ 87.81 (C_6H_6). IR (KBr, cm^{-1}): 1614.8 ν(C=N), 824.2 ν(P-F). Anal. Calcd. for $[C_{18}H_{15}Cl_2N_2Ru]PF_6$ C, 37.52; H, 2.62; N, 4.86. Found: C, 37.70; H, 2.70; N 4.86. MS (ESI, M/Z): 430.9656 $[C_{18}H_{15}Cl_2N_2Ru]^+$

3 $[C_{18}H_{15}ClBrN_2Ru]PF_6$

Yellow powder, yield 80%, m.p. 200.2 °C (decomp.). ^{1}H NMR (600 MHz, DMSO- d_6): δ 9.66 (d, J_{HH} = 5.28 Hz, 1H, H^1), δ 8.91(s, 1H, H^6), δ 8.32 (m, 2H, H^2 , H^4), δ 7.89 (t, J_{HHH} = 8.24 Hz 1H, H^3), δ 7.83 (d, J_{HH} = 8.46 Hz , 2H, H^8, H^{12}), δ 7.76 (d, J_{HH} = 8.64 Hz, 2H, H^9, H^{11}), δ 5.97 (s, 6H, C_6H_6). ^{13}C NMR (400 MHz, DMSO- d_6): δ 169.09 (C^6); δ 156.06 (C^1); δ 151.39 (C^5); δ 140.60 (C^4); δ 132.92 (C^3); δ 130.69 (C^2); δ 129.40 (C^7); δ 125.08 (C^8, C^{12}); δ 123.06 (C^9, C^{11}); δ 87.28 (C_6H_6). IR (KBr, cm^{-1}): 1613.9 ν(C=N), 823 ν(P-F). Anal. Calcd. for $[C_{18}H_{15}ClBrN_2Ru]PF_6$: C, 34.88; H 2.44; N, 4.51. Found: C, 35.38, H 3.07; N 4.49. MS (ESI, M/Z): 477.9146 $[C_{18}H_{15}ClBrN_2Ru]^+$

4 $[C_{18}H_{15}ClIN_2Ru]PF_6$

Orange powder, yield 82%, m.p: 206.8 °C (decomp.). ^{1}H NMR (400 MHz, DMSO- d_6): δ 9.66 (d J_{HH} = 5.40 Hz, 1H, H^1), δ 8.90 (s, 1H, H^6), δ 8.32 (m, 2H, H^2 , H^4), δ 7.99 (d, J_{HH} = 8.36 Hz, 2H, H^3, H^8), δ 7.89 (m, 1H, H^{12}), δ 7.61 (d, J_{HH} = 8.4 Hz , 2H, H^9, H^{11}), δ 5.96 (s, 6H, C_6H_6). ^{13}C NMR (400 MHz, DMSO- d_6): δ 168.31 (C^6); δ 156.28 (C^1); δ 154.55 (C^5); δ 151.29 (C^4); δ 140.07 (C^3); δ 138.22 (C^2); δ 130.13 (C^7); δ 128.84 (C^8, C^{12}); δ 124.53 (C^9); δ 96.07 (C^{11}); δ 87.28 (C_6H_6). IR (KBr, cm^{-1}): 1614.3 ν(C=N), 822.3 ν(P-F). Anal. Calcd. for $[C_{18}H_{15}ClIN_2Ru]PF_6$: C, 32.30; H, 2.26; N, 4.20. Found: C, 31.80, H 2.18; 4.12. MS (ESI, M/Z): 522.8999 $[C_{18}H_{15}ClIN_2Ru]^+$

5 $[C_{18}H_{14}Cl_3N_2Ru]PF_6$

Brown powder, yield 76%, m.p. 224.7 °C (decomp.). ^{1}H NMR (400 MHz , DMSO- d_6): δ 9.64 (d, J_{HH} =5.40 Hz, 1H, H^1), δ 9.06 (s, 1H, H^6), δ 8.37 (s, 2H, H^2 , H^4), δ 7.96 (s, 1H, H^3), δ 7.88 (d, J_{HH} = 8.4 Hz, 1H, H^{12}), δ 7.80 (d, J_{HH} = 2.16 Hz, 1H, H^9), δ 7.69 (m, 1H, H^{11}), δ 6.03 (s, 6H, C_6H_6). ^{13}C NMR (400 MHz, DMSO- d_6): δ 174.61 (C^6); δ 154.02 (C^1); δ 150.14 (C^5); δ 140.88 (C^4); δ 132.96 (C^3); δ 132.66 (C^2); δ 131.80 (C^7); δ 130.67 (C^9); δ130.27 (C^{10}); δ 124.2 (C^8, C^{12}) δ 87.83 (C_6H_6). IR (KBr, cm^{-1}): 1620.6 ν(C=N), 821.1 ν(P-F). Anal. Calcd. for $[C_{18}H_{14}Cl_3N_2Ru]PF_6$: C, 35.60; H, 2.31; N, 4.59. Found: C, 36.06; H, 1.86; N, 4.12. MS (ESI, M/Z): 466.9251 $[C_{18}H_{14}Cl_3N_2Ru]^+$

2.2 General procedure for the synthesis of $[(\eta^6$- *p*-cymene)RuCl(C_5H_4N-2-CH=N-R)]PF_6 6-10

To a suspension of $[(\eta^6$-*p*-cymene)Ru(μ-Cl)]Cl]$_2$ (0.163 mmol) in acetonitrile (10 ml) the ligand **a-e** in slight excess (0.33 mmol) was added. The reaction mixture was stirred for four hours. The solvent was then evaporated and the solid residue treated with NH_4PF_6 (0.35 mmol) in 10 ml of EtOH. The mixture was then stirred in an ice bath for two hours and the solid formed was

collected by filtration, washed with diethyl ether and dried *in vacuo*. The yield and characterization data are given below.

6 $[C_{22}H_{23}ClN_2FRu]PF_6$

Orange powder, yield 82%, m.p. 140.5 °C $_{(decomp.)}$. ^{1}H NMR (400 MHz, DMSO-d_6): δ 9.58 (d, J_{HH} =5.4 Hz, 1H, H^1); 8.91 (s, 1H, H^6); 8.34 (m, 1H, H^2); 8.29 (m, 1H,H^4); 7.91 (m, 3H, H^3, H^8, H^{12}); 7.50 (t, 2H, H^9, H^{11}), 6.09 (d, J_{HH} = 6.78 Hz, 1H, *p*-Cy_{Ar}); 5.78 (d, J_{HH} = 6.42 Hz, 1H, *p*-Cy_{Ar}); 5.70(d, J_{HH} = 6.0 Hz, 1H, *p*-Cy_{Ar}); 5.60 (d, J_{HH} = 6.48 Hz 1H, *p*-Cy_{Ar}), 2.57 (m, 1H, CH $(Me)_2$); 2.17 (s, 3H, *p*-Cy_{Me}); 1.01 (m, 6H, *p*-Cy_{Me}). ^{13}C NMR (400 MHz, DMSO-d_6). δ 168.06 (C^6), δ 159.97 (C^1), δ 154.40 (C^{10}); δ 148.12 (C^5); δ 139.94 (C^4); δ 130.07 (C^3); δ 128.93 (C^2); δ 124.78 (C^7); δ 124.69 (C^8); δ 116.52 (C^{12}) ; δ 105.13 (C^9); δ 103.64 (C^{11}); δ 86.6 (*p*-Cy_{Ar}); δ 86.04 (*p*-Cy_{Ar}); δ 84.9 (*p*-Cy_{Ar})); δ 84.79 (*p*-Cy_{Ar})) ; δ 30.4 (*p*-Cy_{iPro}); δ 21.7 (*p*-Cy_{Me}); δ 21.5 (*p*-$Cy_{Me)}$; δ 18.2 (*p*-Cy_{Me}). IR (solid state): 1610.0 cm^{-1} ν(C=N); 829.9 cm^{-1} ν(P-F). Anal. Calcd. for $[C_{22}H_{23}ClN_2FRu]PF_6$: C, 40.57; H, 3.56; N, 4.30. Found: C, 40.60; H, 3.79; N, 4.51. MS (ESI, M/Z): 471.0580 $[C_{22}H_{23}ClN_2FRu]^+$

7 $[C_{19}H_{20}ClN_2Ru]PF_6$

Brown powder, yield 85%, m.p. 161.0 °C $_{(decomp.)}$. ^{1}H NMR (400 MHz, DMSO-d_6). δ 9.61 (d, J_{HH} = 5.52 Hz, 1H, H^1); 8.91(s, 1H, H^6); 8.34 (m, 2H, H^2,H^4); 7.91 (m, 1H, H^3); 7.86 (m, 2H, H^8,H^{12}), 7.72 (m, 2H, H^9,H^{11}), 6.11 (d, J_{HH} = 6.18 Hz, 1H, *p*-Cy_{Ar}); 5.80 (d, J_{HH} = 6.18 Hz, 1H, *p*-Cy_{Ar}); 5.73 (d, J_{HH} = 6.12 Hz, 1H, *p*-Cy_{Ar}); 5.61(d, J_{HH} = 6.18 Hz, 1H, *p*-Cy_{Ar}); 2.57 (m, 1H, CH $(Me)_2$); 2.18 (s, 3H, *p*-Cy_{Me}); 1.01 (m, 6H, *p*-Cy_{Me}). ^{13}C NMR (400 MHz, DMSO-d_6). δ 168.46 (C^6), δ 156.02 (C^1), δ 154.37 (C^{10}); δ 150.41 (C^5); δ 139.95 (C^4); δ 134.05 (C^3); δ 130.05 (C^2) ; δ 129.55 (C^7) ; δ 129.03 (C^8); δ 124.33(C^{12}) ; δ 105.17 (C^9) ; δ 103.82 (C^{11}); δ 86.68 (*p*-Cy_{Ar}); δ 86.00 (*p*-Cy_{Ar}); δ 84.80 (*p*-Cy_{Ar}); δ 84.73 (*p*-Cy_{Ar}), δ 30.46 (*p*-Cy_{iPro}); δ 21.72 (*p*-Cy_{Me}); δ 21.57 (*p*-Cy_{Me}); δ 18.28 (*p*-$Cy_{Me)}$. IR (solid state): 1615.3 cm^{-1} ν(C=N), 817.9 cm^{-1} ν (P-F). Anal. Calcd. for $[C_{19}H_{20}ClN_2Ru]PF_6$: C, 40.63; H, 3.87; N, 4.31. Found: C, 40.40; H, 3.79 H; N 4.37. MS (ESI, M/Z): 487.0284 $[C_{19}H_{20}ClN_2Ru]^+$

8 $[C_{22}H_{23}Cl_2N_2Ru]PF_6$

Yellow powder, yield 82%, m.p. 184.7 °C $_{(decomp.)}$. ^{1}H NMR (400 MHz, DMSO-d_6). δ 9.58 (d, J_{HH} = 5.4 Hz, 1H, H^1); 8.92 (s, 1H, H^6); 8.33 (m, 2H, H^2,H^4); 8.02 (d, J_{HH} = 8.34 Hz , 2H, H^3, H^8); 7.90 (s, 1H, H^{12}); 7.62 (d, J_{HH} = 8.64 Hz 2H, H^9, H^{11}), 6.10 (d, J_{HH} = 6.18 Hz, 1H, (*p*-Cy_{Ar})); 5.78 (d, J_{HH} = 6.18 Hz, 1H, (*p*-Cy_{Ar})); 5.71 (d, J_{HH} = 6.18 Hz 1H, (*p*-Cy_{Ar})); 5.59 (d, J_{HH} = 6.24 Hz, 1H, (*p*-Cy_{Ar})), 2.56 (m, 1H, CH $(Me)_2$); 2.17 (s, 3H, (*p*-Cy_{Ar})); 1.01 (m, 6H, (*p*-Cy_{Ar})). ^{13}C NMR (400 MHz, DMSO-d_6). δ 168.41 (C^6), δ 156.02 (C^1), δ 154.03 (C^{10}); δ 150.81 (C^5); δ 139.97 (C^4); 132.48 (C^3); δ 130.26 (C^2); δ 129.04 (C^7); δ 124.58 (C^8); δ 122.67 (C^{12}); δ 105.13 (C^9) ; 103.90 (C^{11}); δ 86.72 (*p*-Cy_{Ar}); δ 86.01 (*p*-Cy_{Ar}); δ 84.79 (*p*-Cy_{Ar}); δ 84.71 (*p*-Cy_{Ar}); δ 30.50 (*p*-Cy_{iPro}); δ 21.73 (*p*-Cy_{Me}); δ 21.60 (*p*-Cy_{Me}); δ 18.3 (*p*-Cy_{Me}). IR (solid state): 1613.9

cm^{-1} ν(C=N) 818.1 cm^{-1} ν (P-F). Anal. Calcd. for $[C_{22}H_{23}Cl_2N_2Ru]PF_6$: C, 39.04; H, 3.43; N, 4.14. Found. C, 39.19; H, 3.46; N 3.85. MS (ESI, M/Z): 530.9761 $[C_{22}H_{23}BrClN_2Ru]^+$

9 $[C_{22}H_{23}ClIN_2Ru]PF_6$

Orange powder, yield: 80%, m.p. 204.5°C $_{(decomp.)}$.^{1}H NMR (400 MHz, DMSO-d_6). δ 9.59 (d, J_{HH} = 5.46 Hz, 1H, H^1); 8.93 (s, 1H, H^6); 8.33 (m, 2H, H^2,H^4); 7.92 (m, 1H, H^{12}); 7.87(d, J_{HH} = 8.40 Hz, 2H, H^3, H^8); 7.78(d, J_{HH} = 8.48 Hz, 2H, H^9, H^{11}); 6.11 (d, J_{HH} = 6.36 Hz,1H, (*p*-Cy_{Ar})); 5.79 (d, J_{HH} = 6.42 Hz, 1H, (*p*-Cy_{Ar})); 5.72 (d, J_{HH} = 6.3 Hz, 1H, (*p*-Cy_{Ar})), 5.60 (d, J_{HH} = 6.12 Hz, 1H, (*p*-Cy_{Ar})); 2.57 (m, 1H, CH $(Me)_2$); 2.18 (s, 3H, (*p*-Cy_{Me})); 1.01 (m, 6H, (*p*-Cy_{Me})). ^{13}C NMR δ (400 MHz, DMSO-d_6). δ 168.18 (C^6), δ 156.01 (C^1), δ 154.03 (C^{10}); δ 151.26 (C^5); 139.95 (C^4); 138.28 (C^3); δ 130.23 (C^2); δ 129.00 (C^7); δ 124.55 (C^8); δ 105.07 (C^{12}); δ 103.90 (C^9) ; δ 96.20 (C^{11}); δ 86.70 (*p*-Cy_{Ar}); δ 86.04 (*p*-Cy_{Ar}); δ 84.70 (*p*-Cy_{Ar}); δ 84.67 (*p*-Cy_{Ar}); δ 30.47 (*p*-Cy_{iPro}); δ 21.73 (*p*-Cy_{Me}); δ 21.57 (*p*-Cy_{Me}); δ 18.30 (*p*-Cy_{Me}). IR (solid state): 1614.9cm^{-1} ν(C=N), 815.8cm^{-1} ν(P-F). Anal. Calcd. for $[C_{22}H_{23}ClIN_2Ru]PF_6$: C, 34.80; H, 3.58; N, 3.69. Found: C, 34.65; H, 3.38 H; N, 3.45. MS. (ESI, M/Z): 578.96 $[C_{22}H_{23}ClIN_2Ru]^+$

10 $[C_{22}H_{22}Cl_3N_2Ru]PF_6$

Orange, yield 78%, m.p. 210.4°C $_{(decomp.)}$. ^{1}H NMR (400 MH_Z, DMSO-d_6). δ 9.67 (d, J_{HH} = 5.4 Hz, 1H, H^1); 9.08 (s, 1H, H^6); 8.37 (d, J_{HH} = 7.28 Hz, 2H, H^2, H^4); 7.99 (m, 1H, H^3); 7.88 (m, 2H, H^9, H^{10}), 7.68 (m, 1H, H^{12}); 6.07 (d, J_{HH} = 6.28 Hz, 1H, (*p*-Cy_{Ar})); 5.83 (d, J_{HH} = 6.32 Hz, 1H (*p*-Cy_{Ar})); 5.80 (d, J_{HH} = 6.2 Hz, 1H, (*p*-Cy_{Ar})), 5.50 (d, J_{HH} = 6.12 Hz, 1H, (*p*-Cy_{Ar})), 2.64 (m, 1H, CH $(Me)_2$); 2.09 (s, 3H, (*p*-Cy_{Me})); 1.028 (d, J_{HH} = 6.88 Hz, 3H, (*p*-Cy_{Me}); 0. 94 (d, J_{HH} = 6.88 Hz, 3H, (*p*-Cy_{Me}). ^{13}C NMR (400 MH_Z, DMSO-d_6). δ 173.64 (C^6), δ 156.37 (C^1), δ 153.55 (C^{11}); δ 149.41 (C^5); δ 140.33 (C^4); 132.37 (C^3); δ 132.22 (C^2); δ 130.18 (C^7); δ 130.05 (C^9); δ 124.11 (C^{10}); δ 106.38 (C^8) ; 101.63 (C^{12}); δ 87.04 (*p*-Cy_{Ar}); δ 85.83(*p*-Cy_{Ar}); δ 83.9 (*p*-Cy_{Ar}); δ 30.47 (*p*-Cy_{iPro}); δ 21.74 (*p*-Cy_{Me}); δ 21.20 (*p*-Cy_{Me}); δ 18.07 (*p*-Cy_{Me}). IR (solid state): 1612.1 cm^{-1} ν(C=N); 828.6 cm^{-1} ν (P-F). Anal. Calcd. for $[C_{22}H_{22}Cl_3N_2Ru]PF_6$: C, 39.53; H, 3.33; N, 4.20. Found. C, 39.1; H, 3.64; N, 4.19 MS (ESI, M/Z): 520.9882 $[C_{22}H_{22}Cl_3N_2Ru]^+$

2.3 X-ray crystallography

Crystals for **7(I)** were grown by the slow evaporation method. Crystals of compounds **7(II)** and **10** suitable for x-ray diffraction studies were grown by the solvent diffusion method, where solutions of the compounds in dry acetone were layered with a fourfold excess of hexane and allowed to stand undisturbed in the dark at ambient temperature for 2 days. Crystals of the salts **7(I), 7(II)** and **10e** were selected and glued onto the tip of glass fibres. The crystals were then mounted in a stream of cold nitrogen at 100(1) K and centred in the x-ray beam by using a video camera. The crystal evaluation and data collection were performed on a Bruker Smart *APEX*II diffractometer to crystal distance of 4.00 cm. The initial cell matrix was obtained from three

series of scans at different starting angles. Each series consisted of 12 frames collected at intervals of 0.5 ˚ in a 6˚ range with the exposure time of about 10 s per frame. The reflections were successfully indexed by an automated indexing routine built into the *APEX* II programme suite [30] . The final cell constants were calculated from a set of 6460 strong reflections from the actual data collection. The data collection method involved ω scans of width 0.5˚. Data reduction was carried out using the programme SAINT^{+} [30] . The structure was solved by direct methods using SHELXS [31] and refined by SHELXL [30]. Non-H atoms were positioned geometrically and allowed to ride on their respective parent atoms. All H atoms were refined isotropically. The absorption correction was based on fitting a function to the empirical transmission surface as sampled by multiple equivalent measurements [30]. Crystal data and structure refinement information for compounds **7(I), 7(II)** and **10e** are summarized in **Table 1**.

Table 1. Summary of the crystal data of **7(I), 7(II)** and **7e**

Compound	**7(I)**	**7(II)**	**7e**
Formula	$C_{22}H_{23}Cl_2F_6N_2PRu$	$C_{25}H_{29}Cl_2F_6N_2OPRu$	$C_{22}H_{22}Cl_3F_6N_2PRu$
Formula weight	632.27	690.44	666.80
Crystal system	Orthorhombic	Triclinic	Monoclinic
Space group	Pbcn	$P\bar{1}$	$P2_1/n$
a, Å	16.221(3)	8.967(2)	15.0341(4)
b, Å	20.5555(5)	12.585(3)	10.3961(3)
c, Å	14.3898(18)	12.867(3)	16.9722(3)
α°	90	90	89.086(2)
β°	90	87.935(3)	75.128(2)
γ°	90	74.251(6)	79.328(2)
Cell volume, Å^3	4798.03(18)	1351.4(6)	2471.74(12)
Z	8	2	4
D_{calcd}, Mg/m^3	1.751	1.697	1.792
T, K	173(2)	173(2)	173(2)
μ, mm^{-1}	2.534	3.235	2.534
Wavelength, Å	0.71073	0.71073	0.71073
F(000)	2528	696	1328
Cryst size, mm^3	0.12 x 0.16 x 0.6	0.257 x 0.188 x 0.158	0.180 x 0.140 x 0.097
θ_{min}, θ_{max},°	9.638 to 99.568	1.637 to 26.878	1.553 to 28.473
No. of reflns. collected	140029	4543	55748
No of indep. Reflns.	5627[R(int)]= 0.0809]	4409[R(int)] = 0.0261]	6212[R(int)]= 0.0180]
Completeness to theta	100%	100%	100%
Absorbed correction	Semi-empirical from	Semi-empirical from	Semi-empirical from

	equivalents	equivalents	equivalents
Goodness-of-fit on F^2	1.063	1.039	1.065
Final R indices	0.116, 0.0809	0.0434, 0.1235	0.0196, 0.0486
R indices (all data)	0.1292, 0.0727	0.0457, 0.1266	0.0234, 0.0510
Largest diff.peak & hole, $Å^{-3}$	1.30 & -1.05	1.055 & -2.064	0.607 & -0.448

2.4 Styrene oxidation reaction

All catalytic reactions were performed in a Schlenk tube in an oil bath maintained at 60 ˚C. All products were analyzed using a Perkin Elmer Auto system gas chromatograph fitted with a flame ionization detector (FID) set at 290 ˚C. A Varian wax capillary column (25 mm x 0.15 mm x 2 μm) was utilized with the injector temperature set at 50 ˚C. The substrate to catalyst ratio was set at 1:100. Benzophenone was used as an internal standard. The identity of the products was assessed by comparing their retention times with commercially available (Sigma Aldrich) standards, supported by GC-MS analysis.

2.4.1 General procedure for catalytic oxidation of styrene

Styrene (0.5 mmol), the catalyst (1 mol %) and internal standard (0.5 mmol) were dissolved in a 1:1 mixture of water and *tert*-butanol (6 ml). $NaIO_4$ (4 equivalents) was then added as one portion and the two immiscible solutions were vigorously stirred, in an oil bath, with the temperature maintained at 60 ˚C. The resultant solution was sampled at intervals, whereby an aliquot was removed hourly and 1 μL was injected and analyzed by GC. Control experiments in the absence of either the catalyst or $NaIO_4$ were performed under identical conditions.

3.0 Results and Discussion

3.1 Synthesis and characterization of cationic iminopyridyl Ru(II)-arene complexes.

The reactions of the bimetallic arene precursors $[(\eta^6\text{-arene})Ru(\mu\text{-}Cl)Cl]_2$ with the N,N-bidentate ligands in dry acetonitrile at ambient temperatures give the new mononuclear complexes $[(\eta^6\text{-arene})RuCl(C_5H_4N\text{-}2\text{-}CH{=}N\text{-}R)]^+$ (R = 4-chlorophenyl, 4-bromophenyl, 4-iodophenyl, 4-flourophenyl, 2, 5-dichlorophenyl), which were isolated as their hexafluorophosphate salts (**Scheme 1**). The complexes formed are air-stable and non-hygroscopic. The complexes are soluble in polar solvents such as acetone, acetonitrile, DMSO and DMF, but are insoluble in non-polar solvents such as hexane and diethyl ether.

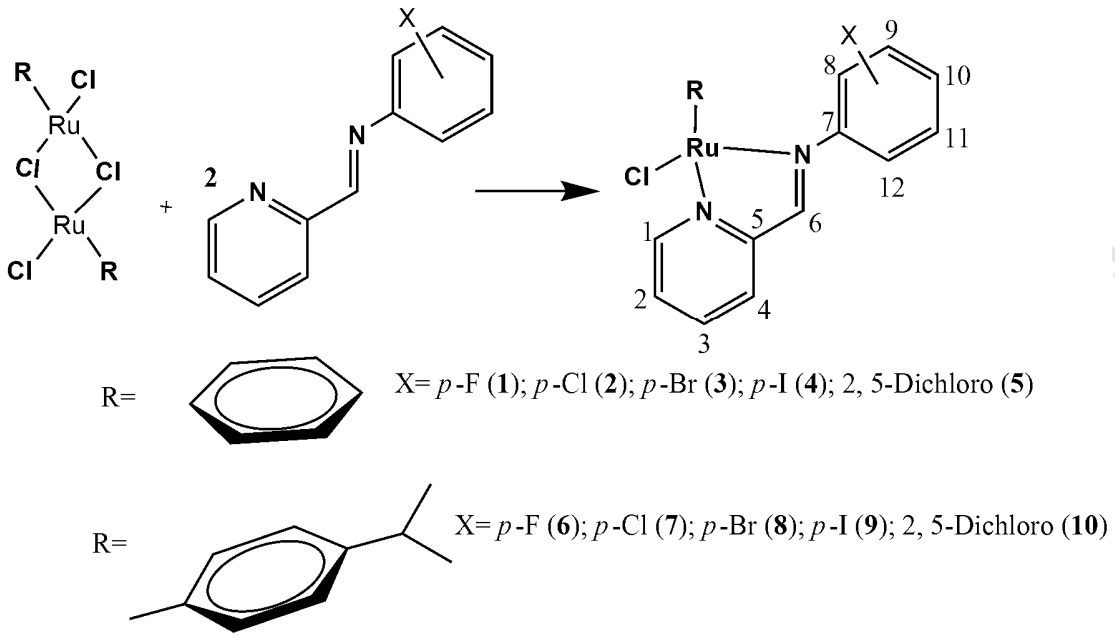

Scheme 1: Synthesis of [(η^6-arene)RuCl(C_5H_4N-2-CH=N-R) PF_6 (arene = C_6H_6 (**1-5**) or *p*-cymene (**6-10**)

The formation of complexes **1** to **5** was confirmed by ^1H and ^{13}C NMR by monitoring the imine proton and carbon signals in the ligand and the complex. The imine proton (γ (CH=N)) shifts downfield to the region δ = 8.90 to 9.10 from the region of δ 8.57 to 8.59 of the free ligand (**Table 2**). This shift can be attributed to the deshielding of the imine proton as the nitrogen atoms donate their lone pair to the metal [32]. In addition, ^{13}C NMR spectra also supported the formation of the complexes. The imine carbon shifted from the region δ 160.1 to 164.2 for the free ligands to the region of 168.3 to 169.1 for the complexes, and this observation was in a good agreement with related compounds reported [33]. For the [η^6-C_6H_6)RuCl(L)]PF_6 complexes, the C_6H_6 singlet of these complexes shifted downfield on coordination, when compared to the precursor complex.

Table 2. ^1H NMR and ^{13}C NMR shifts for the imine functionalities for compounds **1a-e** and **2a-e**

Complex	**^1H NMR**		**^{13}C NMR**	
	Ligand	**Complex**	**Ligand**	**Complex**
1	8.57	8.90	161.4	168.3
2	8.58	8.94	160.6	169.1
3	8.59	8.91	160.1	169.1
4	8.56	8.90	162.1	168.8
5	8.56	9.10	164.1	174.6
6	8.57	8.90	161.4	168.4
7	8.58	8.91	160.6	169.5
8	8.59	8.92	160.1	168.4
9	8.56	8.89	162.2	168.6
10	8.56	9.08	164.2	173.6

The formation of the *p*-cymene complexes **6** to **10** was also confirmed by ^{I}H NMR. The binding of the ligands to the *para*-cymene moiety was confirmed by the observation that the resonances of the benzene ring protons of the *p*-cymene resolved to distinct peaks due to desymmetrization of the arene ring upon coordination of the Schiff base at the ruthenium centre. This observation is in good agreement with those of other workers for related compounds [32]. The formation of the complex was also confirmed by the downfield shift of the imine proton γ(CH=N) to δ = 8.89 - 8.91 from δ = 8.57-8.59 for the free ligands' imine peaks. This shift can be attributed to the deshielding of the amine proton as nitrogen donates its lone pair to the metal (**Table 2**). Furthermore, the ^{13}C NMR spectra for the [(η^6-*p*-cymene)RuCl(L)]PF_6 complexes supported the formation of the complexes due to the downfield shift of the imine carbon from δ = 160.1-164.2 for the free pyridine-imine ligands to δ = 168.4 -173.6 for the complexes. This shift can also also be attributed to the deshielding of the imine carbon, which is in agreement with observations reported by other workers for related complexes [32] (**Table 2**).

The IR spectra also support the formation of the complexes. All the complexes show a strong absorption band in the range 1613-1620 cm^{-1}, which can be assigned to the symmetrical vibration of the γ(C=N) bond. The position of the γ(C=N) bond shifted to lower wavenumbers (1610-1620 cm^{-1}) when compared to those of the free pyridine-imine ligand (1622-1627 cm^{-1}) indicating that the ligands are coordinated to the arene moiety (**Table 3**). This is consistent with the increase in the electron density on the ruthenium(II) centre caused by the coordination of the C=N- group, which resulted in increasing the back bonding to the nitrogen and hence a lower γ(C=N) stretching vibration. Similar trends have been well documented for related compounds [33] . A very strong peak is observed for all complexes in the region 818-830 cm^{-1} and another strong peak in the region 555-556 cm^{-1} which is attributed to the PF_6^- counter ion. This assignment for PF_6^- is in agreement with reports by other workers [34,35]

Table 3. Infrared shifts of the imine functionalities for compounds **3a-e** and **4a-e**

Complex	**Ligand** $(C=N)_{pyridine}$	**Complex** $(C=N)_{pyridine}$
1	1624.5	1614.4
2	1623.3	1614.8
3	1622.7	1613.9
4	1627.1	1615.6
5	1625.3	1620.6
6	1624.5	1614.9
7	1623.3	1615.3
8	1622.7	1613.9
9	1627.1	1610.1
10	1625.3	1612.7

High resolution mass spectra were also obtained to confirm the formation of the mononuclear complexes. They all lose the counter anion PF_6^- to give the base peak of the N, N′-bidentate complex $[(\eta^6\text{-arene})RuCl(C_5H_4N\text{-}2\text{-}CH{=}N\text{-}R)]^+$. The characteristic multiple peaks associated with stable isotopes of ruthenium are also observed in each fragment.

The Uv-vis data of the complexes **1** to **5** and **6** to **10 (Figs. 1** and **2)** and their respective ligands were obtained in acetonitrile. Absorption bands were observed in the regions 230 nm -249 and 282 nm-327 nm for the ligands which can be attributed to n-π* and π-π* transitions respectively. These bands underwent a bathochromic shift to 255 - 273 nm and 311-316 nm in the complexes. In addition the complexes presented bands in the regions 410-423 nm which could be assigned to the metal to ligand (dπ-π*) charge transfer (MLCT) transition from the filled 4d orbital to the empty π* orbital. These bands were not observed in the ligand, UV-vis thus further confirming the formation of the complexes. This assignment is in agreement with those of other workers for *N, N'* bidentate ligands [36].

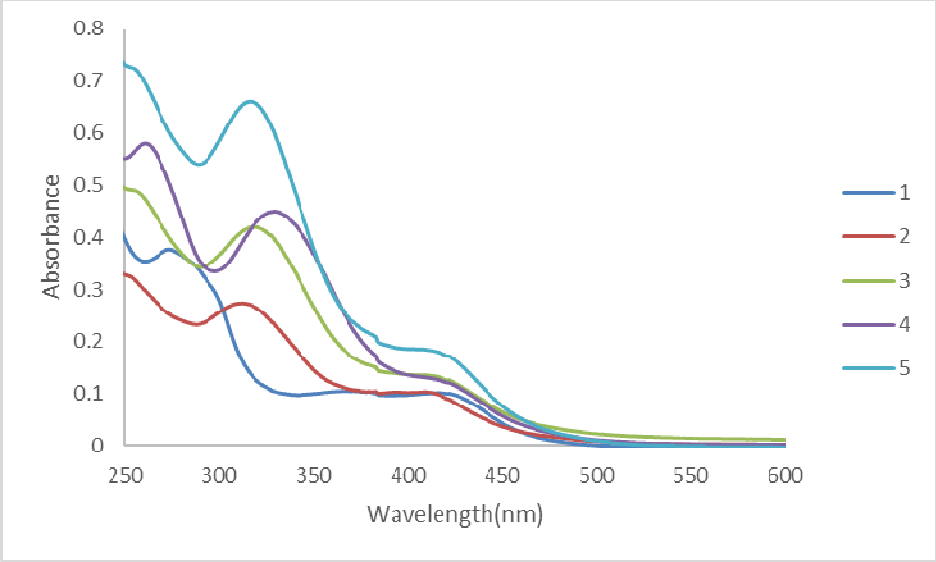

Figure 1: UV-Vis spectra of the complexes **1** to **5**

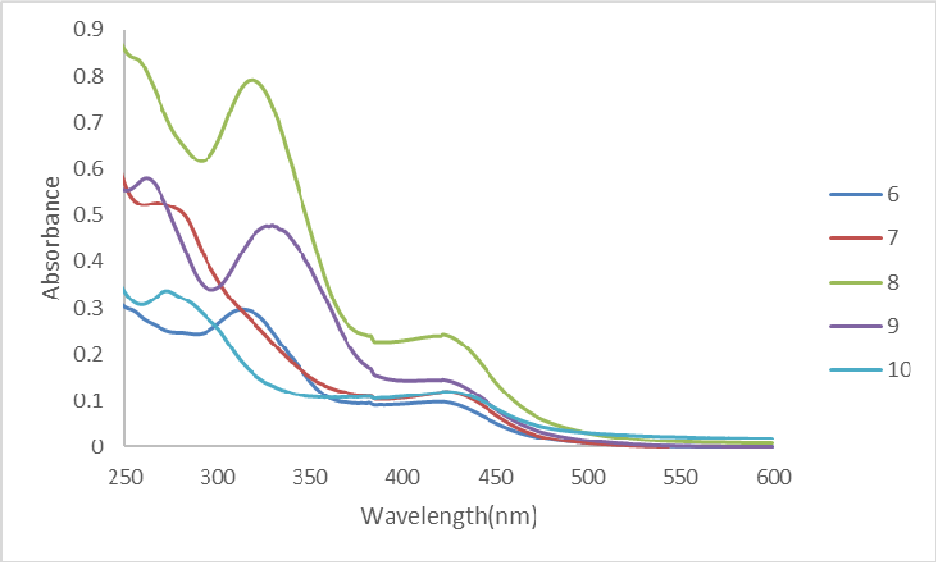

Figure 2: UV-Vis spectra of the complexes **6** to **10**

The TGA data was obtained in the range of 25˚C to 700 ˚C (Figures 3 and 4). The thermograms of the compounds presented two main mass loss steps during the decomposition of the compounds. The first step occurred between 170 and 330 ˚C and the second step occurred between 340 and 510˚C. The first decomposition in all cases reflected a weight loss of approximately 30%, which may be attributed to the loss of the pyridine-imine ligand. The second decomposition step of approximately 20% may be attributed to the loss of the arene ring.

The DSC results for the complexes 1-10 show two endothermic peaks at 180-290 ˚C and 310-450 ˚C. The first peak indicates the compounds undergoes a phase transition on melting and the second peak indicates possible phase transition during which the compound is completely decomposed. This has been observed by other researchers for arene ruthenium compounds [37].

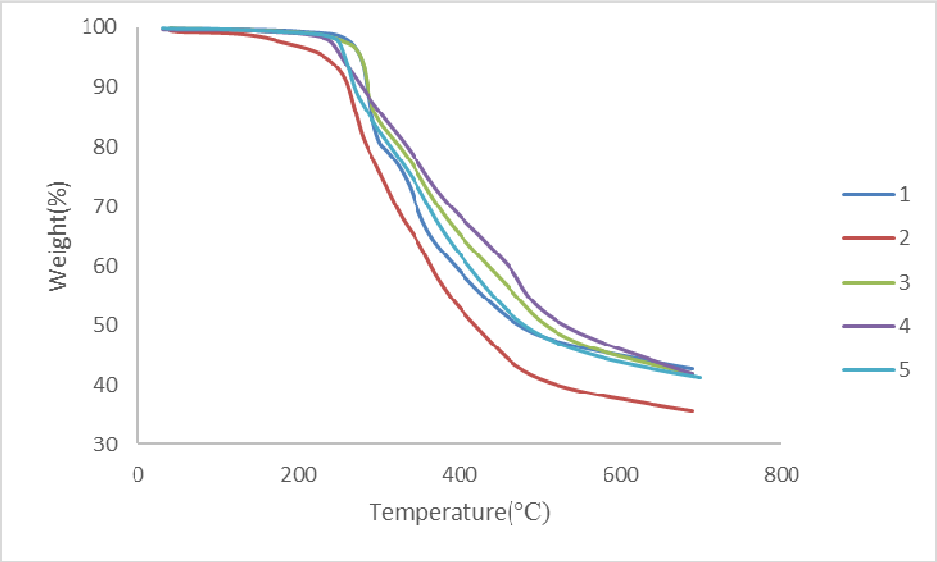

Figure 3: TGA trace of **1-5**

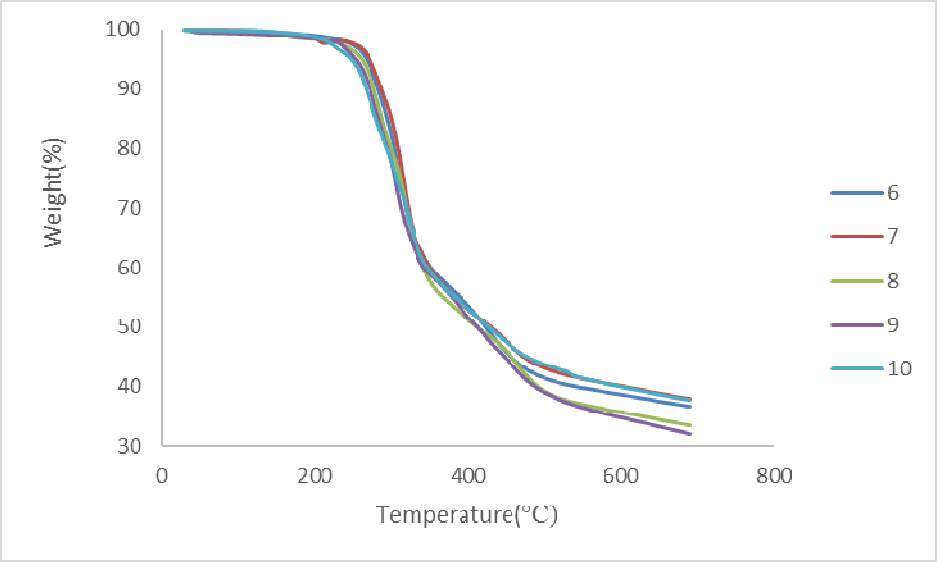

Figure 4: TGA trace of **6-10**

3.2 Crystal and molecular structures

Compounds **7** and **10** crystalize as red block crystals. Single crystal X-ray analysis of these compounds revealed that **7** crystallizes without a solvent molecule, **7(I)** and as an acetone solvate **7(II)**. The molecular structures of the complexes are provided in **Figs. 5, 6** and **7**, while **Table 4** gives a comparison of important bond distances and angles. Whereas **7(I)** crystallizes in the orthorhombic *Pbcn* space group with a molecule of the cation $[(\eta^6\text{-}p\text{-cymene})RuL)]^+$ and two half molecules of the anion PF_6^- in the asymmetric unit, **7(II)** crystallizes in the triclinic $P\bar{1}$ space group with a molecule of acetone in addition to the cation $[(\eta^6\text{-}p\text{-cymene})RuL)]^+$ and two half molecules of the counter anion PF_6^-. Compound **10** on the other hand has the cation and one molecule of the anion in the asymmetric unit. In all three cationic species the substituted N-(pyridin-2-ylmethylene) aniline ligand is coordinated to the Ru(II) center through the N atom of the pyridine and the N atom of the imine bond in a bidentate manner resulting in a five member metallacycle. The geometry around the Ru(II) center is distorted pseudo-octahedral in which the two N atoms and the Cl atoms form the base, while the *p*-cymene rings form the apex of a "three-legged piano stool" structure [38]. All three cations feature two distinct molecular planes described by the pyridine ring including the imine N, and the *para*-substituted phenyl ring. The two planes have a dihedral angle of 50.9(1) in **7(I)**, 52.2(1) in **7(II)** and 55.7(1)° in **10** presumably to reduce steric hindrance caused by the cymene ligand, which is in agreement with reports on related compounds [39]. The Ru-N bond lengths of the three complexes lie between 2.066(3) Å and 2.083(3) Å and are comparable to those reported for similar arene ruthenium complexes with N, N' donor ligands [39,40]. The Ru-N bond lengths also fall within the reported values of half-sandwich complexes of $[(\eta^6\text{-arene})Ru(\mu\text{-}Cl)Cl]_2$ with nitrogen ligands which ranged from 2.060(5) Å to 2.156(2) Å [40]. The N-Ru-N bond angles range from 76.62(5) to 76.78(12) and the N-Ru-Cl bond angles range from 84.46(8) to 85.39(8) ˚. These values are close to those reported for related compounds [40,41].

Table 4: Selected bond lengths (Å) and angles (deg)

7(I)		7(II)		10e	
Bond Lengths		**Bond Lengths**		**Bond Lengths**	
Ru(1)-N(1)	2.103(3)	Ru(1)-N(1)	2.066(3)	Ru(1)-N(1)	2.0799(12)
Ru(1)-N(2)	2.094(3)	Ru(1)-N(2)	2.083(3)	Ru(1)-N(2)	2.0687(12)
Ru(1)-Cl(1)	2.4039(11)	Ru(1)-Cl(1)	2.3641(10)	Ru(1)-Cl(3)	2.3910(4)
N(1)-C(5)	1.364(5)	N(1)-C(15)	1.351(4)	N(2)-C(17)	1.4310(18)
N(1)-C(7)	1.435 (5)	N(1)-C(11)	1.330(3)	N(2)-C(16)	1.2900(19)
Bond angles		**Bond angles**		**Bond angles**	
N(1)-Ru(1)-N(2)	76.70(12)	N(1)-Ru(1)-N(2)	76.78(12)	N(2)-Ru(1)-N(1)	76.62(5)
N(1)-Ru(1)-Cl(1)	85.56(9)	N(1)-Ru(1)-Cl(1)	85.46(8)	N(1)-Ru(1)-Cl(3)	84.52(3)
N(2)-Ru(1)-Cl(1)	85.77(9)	N(2)-Ru(1)-Cl(1)	85.39(8)	N(2)-Ru(1)-Cl(3)	85.06(3)

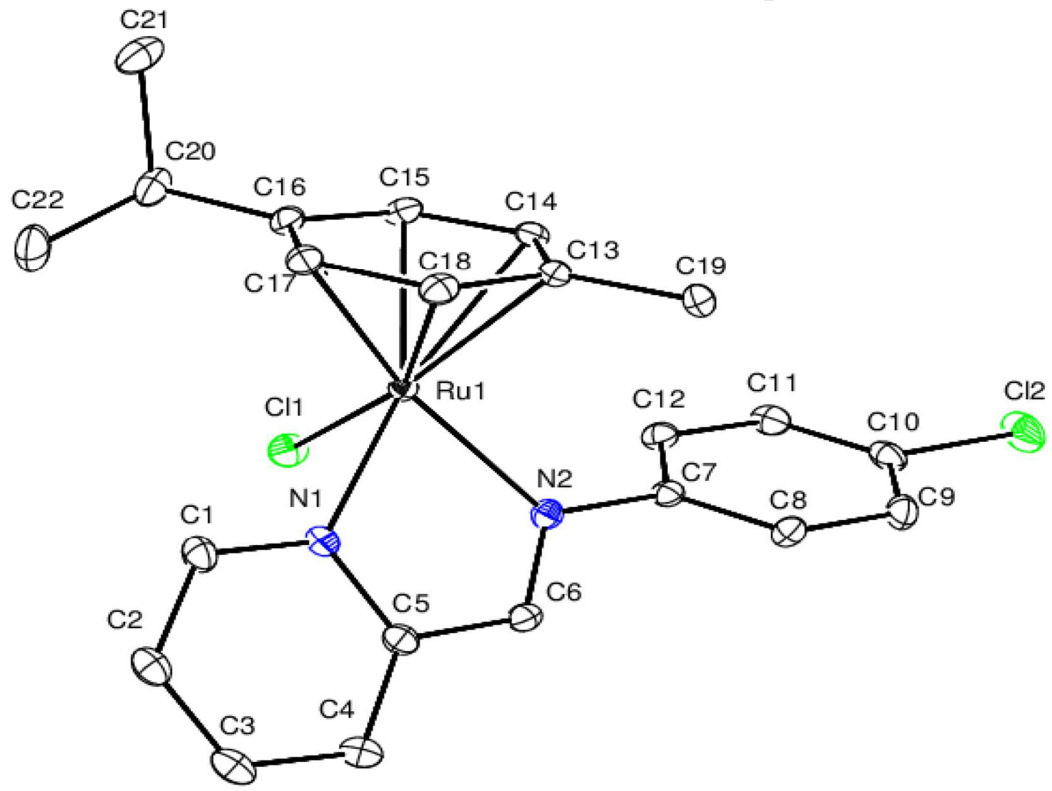

Figure 5. The molecular structure of **7(I)** showing atomic numbering scheme**.** Displacement ellipsoids are drawn at the 50% probability level. The PF_6 counter ion has been omitted for clarity.

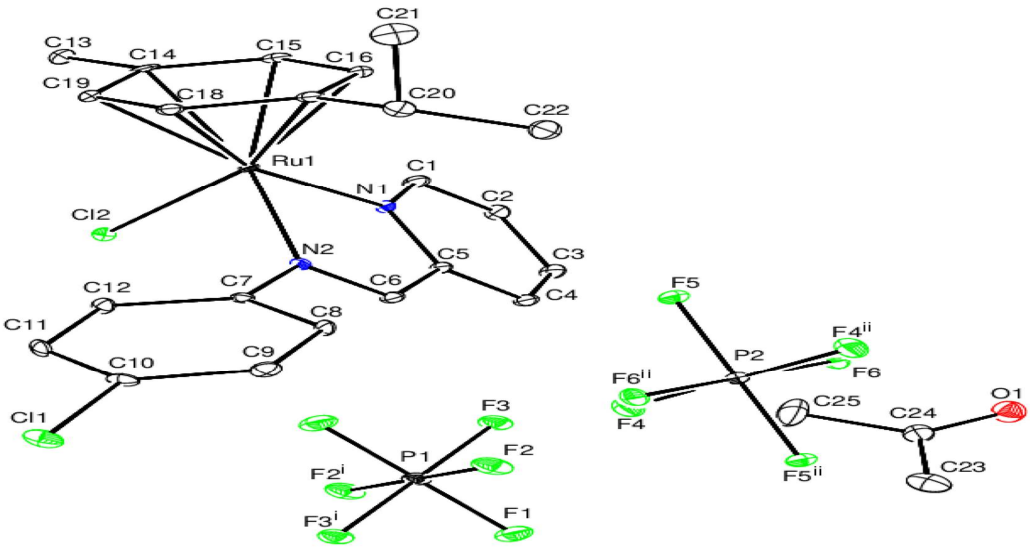

Figure 6. The molecular structure of **7(II)** showing the atomic numbering scheme**.** Displacement ellipsoids are drawn at the 50% probability level.

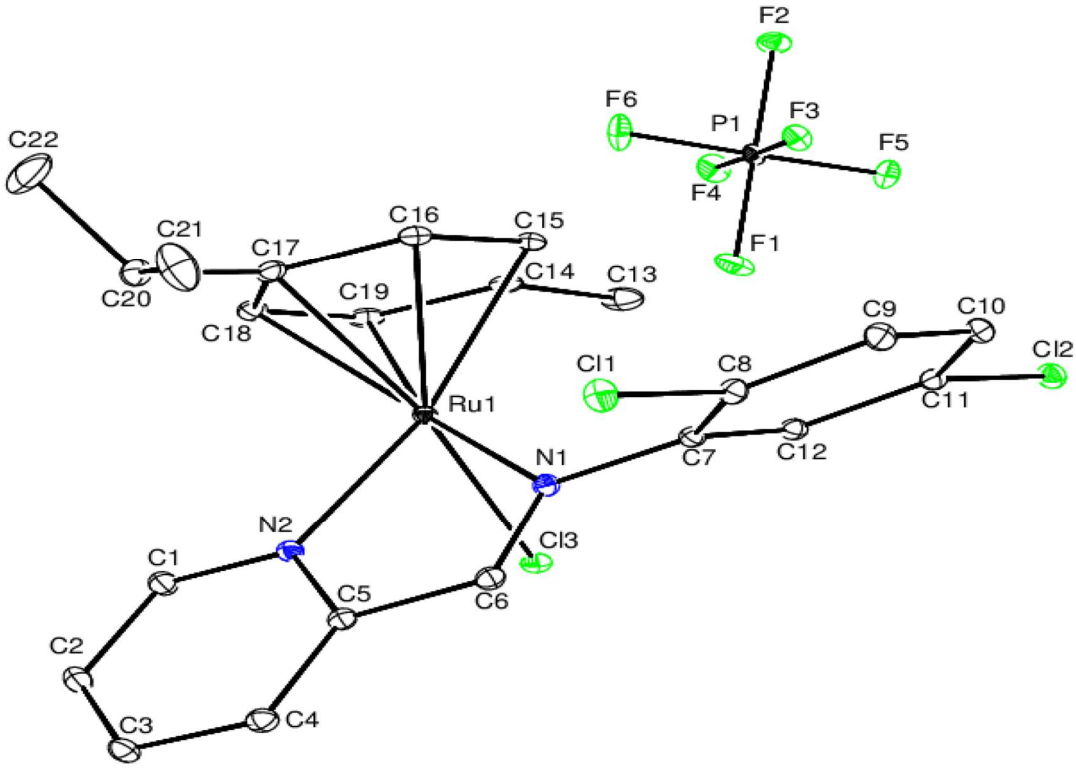

Figure 7. The molecular structure of **10** showing the atomic numbering scheme. Displacement ellipsoids are drawn at the 50% probability level

3.3 Styrene oxidation

3.3.1 Optimization

The effects of the solvent, oxidant, catalyst loading and temperature were investigated in preliminary optimization studies of the half-sandwich ruthenium compound **7** in the catalytic oxidation of styrene. Initially the effect of temperature was investigated, at room temperature, 40 and 60 ˚C. The best conversion of styrene and yield to benzaldehyde was at 60 ˚C and thus this temperature was chosen for the further studies. Next, the effect of the solvent was investigated using acetonitrile, toluene, anisole and *tert*-butanol. The optimum ratio of organic solvent to water was found to be 1:1. In addition, *tert*-butanol was found to be the best solvent giving the highest conversion of styrene and highest selectivity to benzaldehyde.

In addition, three different oxidants were investigated, namely tert-butyl hydroperoxide, oxone and $NaIO_4$. $NaIO_4$ gave the best conversion and selectivity towards benzaldehyde and thus was selected for subsequent reactions. It was found that the best conversion was obtained with 4 equivalents of the oxidant. On increasing the amount of the oxidant beyond 4 equivalents the same conversion of styrene and yield to benzaldehyde was obtained, and on decreasing the ratio a drop in conversion was found. The effect of catalyst loading was also explored by varying the loading from 0.625 mol% to 2.5 mol%. The best catalytic results were achieved when 1 mol% of catalyst was added to the reaction media. A lower amount of added catalysts showed a drop in conversion, while catalyst loading above 1 mol % did not change the conversion and yields.

The best conditions for maximum conversion of styrene to benzaldehyde thus were found to be a 1:1 *tert*-butanol: water ratio; 60 ˚C, 1 mol % catalyst loading and a co-oxidant equivalence of 4%. A series of blank experiments were carried out under identical conditions, which showed that the ruthenium(II) complexes did not give conversions without $NaIO_4$. The oxidant $NaIO_4$ alone gave low conversion without the presence of the catalyst. The final conversions are reported as an average of three runs for each catalytic reaction.

3.3.2 Catalytic results discussion

Previous research on styrene oxidation has demonstrated that oxidation at the side chain can lead to various reaction products, depending on the catalyst and the reaction conditions. Two major reactions take place, namely oxidative C=C cleavage into benzaldehyde and epoxidation [1,42].

Under the present catalysis conditions the major oxidation product was benzaldehyde. This may be attributed to direct oxidative cleavage of C=C of styrene or the fast conversion of styrene oxide to benzaldehyde. The latter route was confirmed by the oxidation of styrene oxide under the same catalytic conditions which showed complete conversion to benzaldehyde.

Complexes **1-5** and **6-10** were then tested for the catalytic oxidation of styrene. Highest conversions were reached after three hours with catalysts **1-4**, one hour with catalysts **5** and **10** (**Figs. 8** and **9**). For catalysts **6-9** the highest conversions were obtained after 2 hours (**Table 6**).

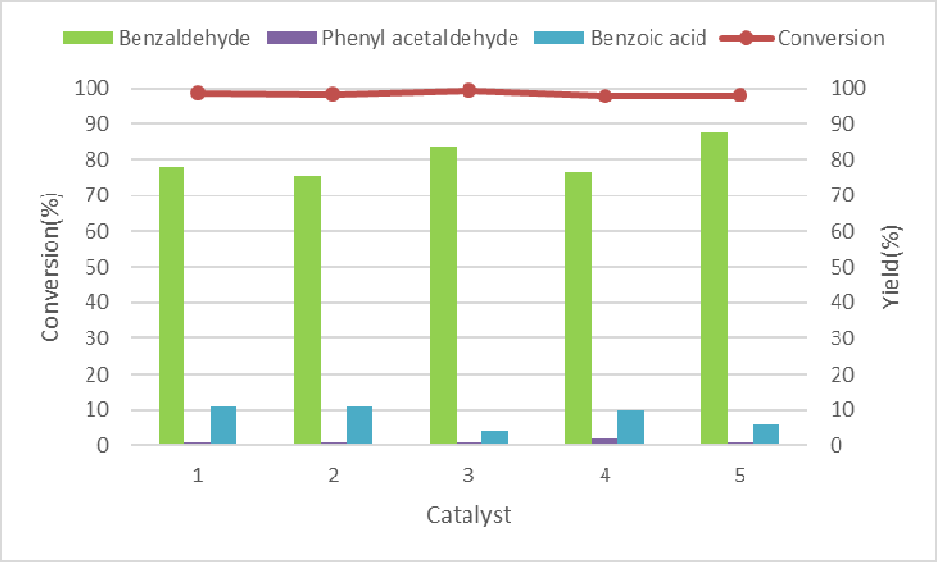

Figure 8. Effect of Substituents on $[(\eta^6\text{-arene})RuCl(C_5H_4N\text{-}2\text{-}CH{=}N\text{-}R)]PF_6$ (arene = C_6H_6 (**1-5**)) on styrene oxidation.

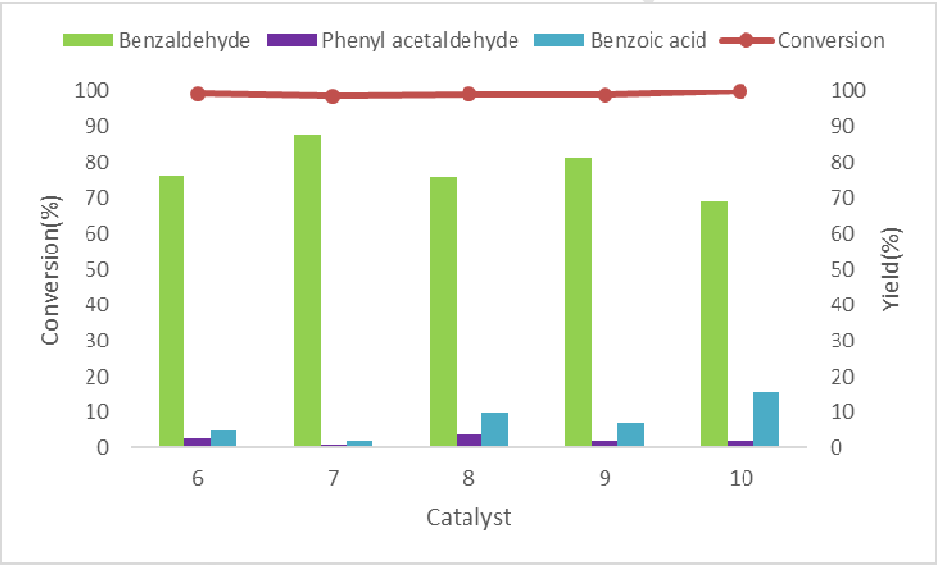

Figure 9. Effect of Substituents on $[(\eta^6\text{-arene})RuCl(C_5H_4N\text{-}2\text{-}CH{=}N\text{-}R)]PF_6$ (arene = *p*-cymene (**6-10**)) on styrene oxidation.

The increase in the byproduct benzoic acid with increase in reaction time implied that it was formed by further reaction of benzaldehyde and the formation of benzaldehyde and phenyl

acetaldehyde might proceeded via parallel pathways. The product specific turn over numbers (TON) and turn over frequencies are shown in **Table 6**.

Table 6. Oxidation of styrene results for catalysts **1**-**5** and **6**-**10**

Catalyst	Major product	Time	TON[a]	TOF[b]
1	benzaldehyde	3	78	26
2	benzaldehyde	3	76	25
3	benzaldehyde	3	84	28
4	benzaldehyde	3	76	25
5	benzaldehyde	1	87	87
6	benzaldehyde	2	76	38
7	benzaldehyde	2	88	44
8	benzaldehyde	2	76	41
9	benzaldehyde	2	81	38
10	benzaldehyde	1	69	69

[a]TON: mol of product/mol of catalyst

[b]TOF: mol of product/(mol. of catalyst x time)

On comparing the effect of changing the arene ring on styrene oxidation, the complexes with p-cymene ligands perform better in terms of time taken to complete the reaction. There was no remarkable effect on changing the ligand substitution, except with the 2, 5- substituted ligand and this could be attributed to the strong electron withdrawing nature of this ligand which may stabilize the intermediate oxo species.

Having established the optimum conditions for the reaction, the study was extended to other olefins aimed at establishing its scope and limitations. For the extended study catalyst **5** was used, since it gave the highest catalytic TON for the respective series. The catalyst showed high conversions for styrene with both electron withdrawing (Cl) group and electron donating groups (Me, OMe), giving the corresponding the aldehyde in very good yields. The catalyst was also able to cleave the bond in trans-stilbene to give benzaldehyde and was active for straight chain alkenes, with 1-octene giving 1-heptanal (**Table 7**).

Table 7: Oxidative cleavage of olefins by **5** with $NaIO_4$

Entry	Substrate	Product	Conversion	Yield	Time	TON	TOF
1	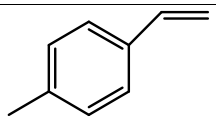	4-methyl benzaldehyde	100	92	0.5	93	186
2	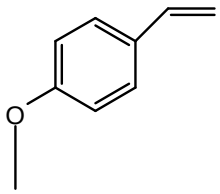	4-methoxy benzaldehyde	98	90	2	86	86
3	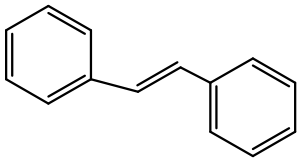	Benzaldehyde	100	93	1	93	93
4	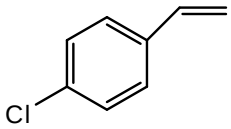	4-chrolo benzaldehyde	100	94	1	94	94
5		1-heptanal	99	91	1	92	92

All the catalyst systems displayed good activity and selectivity to the cleaved product. "Catalyst'' **5** was recycled three cycles with styrene as the substrate without significant loss of activity. A 5% increase in benzoic acid yield was observed and this could be attributed to the species formed after the first catalytic cycle being significantly more active than the original catalyst and thus leading to some over oxidation of the benzaldehyde formed. This implies that the ruthenium(II) arene complex is not the catalyst itself, but a catalyst precursor which forms a more catalytically active intermediate which is not deactivated at the end of the catalytic reaction.

When the catalysts in this study are compared with other reported ruthenium catalysts, they were found to perform better than the Ru-N-heterocyclic carbene compounds reported by Poyatos and coworkers [43], who reported lower conversions 23-58% and longer reaction times (24 hours) for styrene and stilbene derivatives. The catalysts in this study were also better when compared to $[Ru(dmp)_2(H_2O)_2]^{2+}$ (dmp= 2,9-dimethyl phenathroline) which was found to require longer reaction times (up to eight hours) [44]. In addition, these catalyst were also better than a

reported $RuCl_3/NaIO_4$ system by Yang and Zhang, which required high catalyst loading (3.5 mol %) to afford moderate yields of oxidative cleaved products [45]. However, catalysts **1**-**5** and **6**-**10** were found to be less reactive than the system reported by Daw and coworkers who used $[Ru(COD)(L_1)Br_2]$, where L_1 is a fused naphthyridine–based N-heterocyclic carbon ligand, in an $EtOAC/CH_3CN/H_2O$ solvent mixture at room temperature [2]. When these catalysts are compared to η^5-cyclopentadienyl dicarbonyl ruthenium(II) amine complexes [46], the reported catalysts required a lower catalyst loading of 0.5 mol% but also longer reaction times.

On the basis of earlier work [41,46-50] and some observations made in this work, it is suggested that the selective aldehyde formation involves a high valent Ru-oxo species as an intermediate. The mechanism of catalytic oxidation seems to involve Ru(VI)=O species, which formed by free radicals generated by heterolytic cleavage of the oxidants [51]. On the addition of $NaIO_4$ (oxidant) to the tert-butanol solution of **6**, as a model catalyst, a new shoulder at 360 nm appears in its UV-Vis spectrum which is an indication for the presence of Ru(VI)=O species [49]. This value is close to the values reported by other researchers for Ru(VI)=O species and the Ru(VI)=O is the functionality reported to be responsible for transfer of the oxygen. Furthermore, when the solvent from a mixture of $NaIO_4$ with complex **6** was evaporated, the IR spectrum of the remaining residue was found to exhibit strong bands at 813, 764 and 718 cm^{-1} which could be assigned to the symmetric and asymmetric stretching of the Ru=O bonds of the Ru(VI) di-oxo species, which further supports the formation of Ru(VI)=O species responsible for the catalytic oxidation [47]. The ^1H NMR spectrum of the residue showed three peaks in the region δ 6.10 to 5.31 ppm assignable to the Ru(cymene) arene ring. This suggests that the ruthenium moiety containing the coordinated cymene remains after the catalytic run. This observation has been reported also for related compounds [5,46]

Furthermore, the ESI-MS spectra of the residue from the experiment carried out using **6** was obtained. One major species observed containing the Ru fragment showed a peak at 398 (maximum of the isotopic cluster), which may be attributed to $[(p\text{-cymene})RuCl(O_2)(MeCN)(H_2O)_3]^+$. This result suggests that there is in existence in solution a ruthenium species containing coordinated cymene, but also that there is cleavage of the N, N-bidentate ligand. On the basis of the mentioned observations and available literature, a mechanism that involves a Ru(VI) oxo species can be proposed (**Scheme 2**). The catalysts reacts with the terminal oxidant $NaIO_4$ to form a Ru(VI)-cis dioxo intermediate. Then, electrophilic attack on the C=C bond by the high-valent dioxo-intermediate affords a Ru(IV) cyclo adduct via a concerted [3+2] cycloaddition reaction.

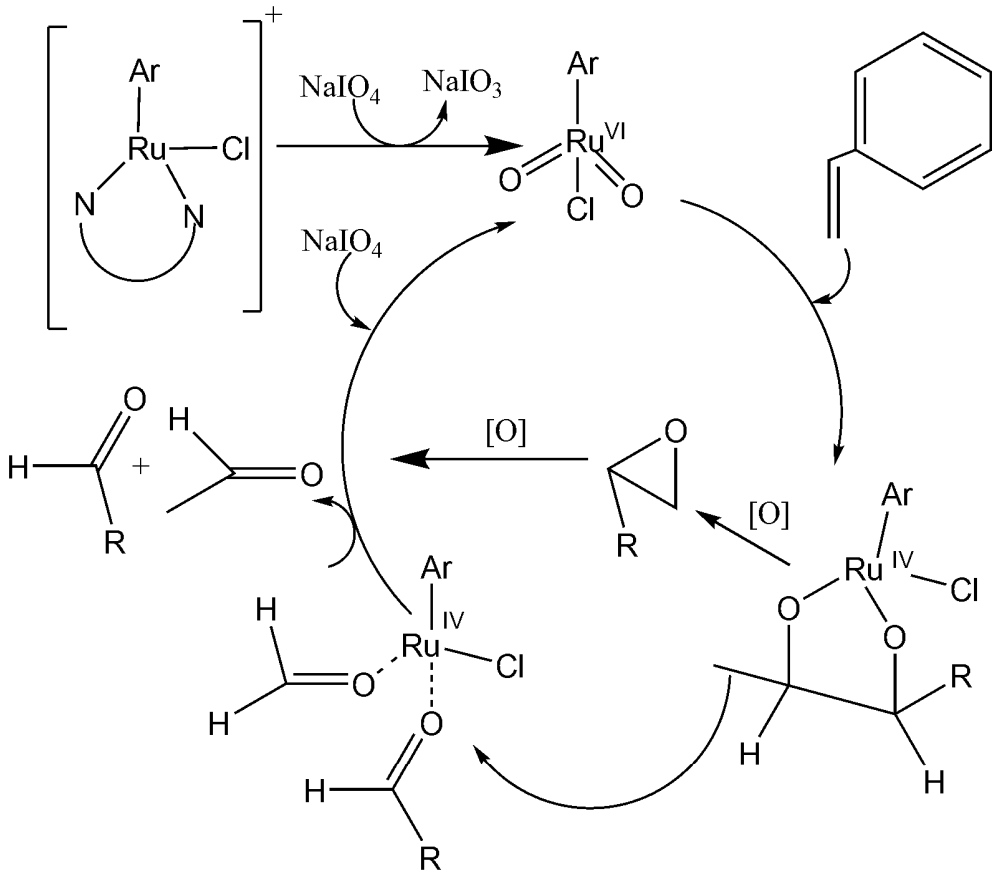

Where Ar = Arene

R= 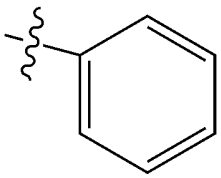

Scheme 2: Proposed mechanism for styrene oxidation using compounds **1**-**10**.

Conclusion

The mononuclear complexes **1** to **5** and **6** to **10** have been successfully synthesized, isolated and characterized. The structures of two of these compounds have been determined by single crystal crystallography. Compound **7** was found to crystallize as two polymorphs, triclinic and orthorhombic, depending on the method of crystal growth. All the complexes showed the pseudo octahedral three legged piano stool geometry. The compounds were found to be very reactive in styrene oxidation with good benzaldehyde selectivity. The major products obtained were benzaldehyde (70-88%) and benzoic acid (5-16%). The oxidative cleavage of other substrates 4-methyl styrene, 4-methoxy styrene, stilbene, 4-chloro styrene and 1-octene gave the

corresponding aldehydes. The proposed mechanism involves a Ru(VI) oxo species as supported by the UV, ^{1}HNMR, ESI-MS and IR spectra.

Supplementary material

CCDC 1432508, 1432426, 1432344 contain the supplementary crystallographic data for this paper. These data can be obtained free of charge via http://www.ccdc.cam.ac.uk/conts/retrieving.html (or from the Cambridge Crystallographic Data Centre, 12, Union Road, Cambridge CB2 1EZ, UK; fax: +44 1223 336033).

Acknowledgement

We wish to extend our sincere thanks to the NRF, THRIP (Grant no. TP 1208035643) and UKZN (URF) for financial support. JG thanks Prof. E. N. Njoka for his support.

REFERENCES

[1] J. Valand, H. Parekh, H.B. Friedrich, Catal. Commun. 40 (2013) 149.
[2] P. Daw, R. Petakamsetty, A. Sarbajna, S. Laha, R. Ramapanicker, J.K. Bera, J. Am. Chem. Soc. 136 (2014) 13987.
[3] T.K. I.W. Arends, R. A. Sheldon, Top. Organomet. Chem. 11 (2004) 277.
[4] S.-I. Murahashi, N. Komiya, Y. Oda, T. Kuwabara, T. Naota, J. Org. Chem. 65 (2000) 9186.
[5] F. Marchetti, C. Pettinari, R. Pettinari, A. Cerquetella, C. Di Nicola, A. Macchioni, D. Zuccaccia, M. Monari, F. Piccinelli, Inorg. Chem. 47 (2008) 11593.
[6] S. Betanzos-Lara, L. Salassa, A. Habtemariam, O. Novakova, A.M. Pizarro, G.J. Clarkson, B. Liskova, V. Brabec, P.J. Sadler, Organometallics 31 (2012) 3466.
[7] R. Noyori, S. Hashiguchi, Acc. Chem. Res. 30 (1997) 97.
[8] J. Canivet, G. Suss-Fink, Green Chem. 9 (2007) 391.
[9] D. Šterk, M.S. Stephan, B. Mohar, Tetrahedron: Asymm. 13 (2002) 2605.
[10] B. De Clercq, F. Verpoort, J. Mol. Catal. A: Chem. 180 (2002) 67.
[11] Á. Kathó, D. Carmona, F. Viguri, C.D. Remacha, J. Kovács, F. Joó, L.A. Oro, J. Organomet. Chem. 593 (2000) 299.
[12] C. Ganesamoorthy, M.S. Balakrishna, J.T. Mague, J. Organomet. Chem. 694 (2009) 3390.
[13] R.K. Rath, M. Nethaji, A.R. Chakravarty, Polyhedron 20 (2001) 2735.
[14] A. Habtemariam, M. Melchart, R. Fernández, S. Parsons, I.D.H. Oswald, A. Parkin, F.P.A. Fabbiani, J.E. Davidson, A. Dawson, R.E. Aird, D.I. Jodrell, P.J. Sadler, J. Med. Chem. 49 (2006) 6858.
[15] Y.K. Yan, M. Melchart, A. Habtemariam, P.J. Sadler, Chem. Commun. (2005) 4764.
[16] R. Fernández, M. Melchart, A. Habtemariam, S. Parsons, P.J. Sadler, Chem. Eur. J. 10 (2004) 5173.
[17] W.F. Schmid, R.O. John, G. Mühlgassner, P. Heffeter, M.A. Jakupec, M. Galanski, W. Berger, V.B. Arion, B.K. Keppler, J. Med. Chem. 50 (2007) 6343.
[18] R.E. Morris, R.E. Aird, P. del Socorro Murdoch, H. Chen, J. Cummings, N.D. Hughes, S. Parsons, A. Parkin, G. Boyd, D.I. Jodrell, P.J. Sadler, J. Med. Chem. 44 (2001) 3616.
[19] G. Ludwig, G.N. Kaluđerović, M. Bette, M. Block, R. Paschke, D. Steinborn, J. Inorg. Biochem. 113 (2012) 77.
[20] É.A. Enyedy, G.M. Bognár, T. Kiss, M. Hanif, C.G. Hartinger, J. Organomet. Chem. 734 (2013) 38.
[21] R.D. Pike, D.A. Sweigart, Coord. Chem. Rev. 187 (1999) 183.
[22] O. Dayan, S. Demirmen, N. Özdemir, Polyhedron 85 (2015) 926.
[23] P. Govindaswamy, Y.A. Mozharivskyj, M. Rao Kollipara, Polyhedron 23 (2004) 1567.
[24] K.S. Singh, P.J. Carroll, M.R. Kollipara, Polyhedron 24 (2005) 391.
[25] S.S. Keisham, Y.A. Mozharivskyj, P.J. Carroll, M.R. Kollipara, J. Organomet. Chem. 689 (2004) 1249.
[26] L.C. Matsinha, P. Malatji, A.T. Hutton, G.A. Venter, S.F. Mapolie, G.S. Smith, Eur. J. Inorg. Chem 2013 (2013) 4318.
[27] M.A. Bennett, A.K. Smith, J. Chem.Soc., Dalton. Trans. (1974) 233.
[28] S. Dehghanpour, A. Mahmoudi, Main Group Chem. 6 (2007) 121.
[29] J. Gómez, G. García-Herbosa, J.V. Cuevas, A. Arnáiz, A. Carbayo, A. Muñoz, L. Falvello, P.E. Fanwick, Inorg. Chem. 45 (2006) 2483.
[30] Bruker-AXS, Bruker-AXS, Madison, Wisconsin, USA, 2009.
[31] G.M. Sheldrick, Acta Crystallogr. A64 (2008) 112.
[32] L.C. Matsinha, S.F. Mapolie, G.S. Smith, Polyhedron 53 (2013) 56.

[33] P. Govender, A.K. Renfrew, C.M. Clavel, P.J. Dyson, B. Therrien, G.S. Smith, Dalton Trans. 40 (2011) 1158.
[34] F. Marchetti, C. Pettinari, A. Cerquetella, A. Cingolani, R. Pettinari, M. Monari, R. Wanke, M.L. Kuznetsov, A.J.L. Pombeiro, Inorg. Chem. 48 (2009) 6096.
[35] S. Orbisaglia, C. Di Nicola, F. Marchetti, C. Pettinari, R. Pettinari, L.M.D.R.S. Martins, E.C.B.A. Alegria, M.F.C. Guedes da Silva, B.G.M. Rocha, M.L. Kuznetsov, A.J.L. Pombeiro, B.W. Skelton, A.N. Sobolev, A.H. White, Chem. Eur. J. 20 (2014) 3689.
[36] S. Gloria, G. Gupta, V. Rao Anna, B. Das, K.M. Rao, J. Coord. Chem. 64 (2011) 4168.
[37] K.-G. Liu, X.-Q. Cai, X.-C. Li, D.-A. Qin, M.-L. Hu, Inorg. Chim. Acta 388 (2012) 78.
[38] P. Kumar, R.K. Gupta, D.S. Pandey, Chem. Soc. Rev. 43 (2014) 707.
[39] M.J. Chow, C. Licona, D. Yuan Qiang Wong, G. Pastorin, C. Gaiddon, W.H. Ang, J. Med. Chem. 57 (2014) 6043.
[40] S.K. Mandal, A.R. Chakravarty, Polyhedron 11 (1992) 823.
[41] P. Singh, A.K. Singh, Organometallics 29 (2010) 6433.
[42] A. Patel, S. Pathan, Ind. & Eng. Chem. Res. 51 (2012) 732.
[43] M. Poyatos, J.A. Mata, E. Falomir, R.H. Crabtree, E. Peris, Organometallics 22 (2003) 1110.
[44] V. Kogan, M.M. Quintal, R. Neumann, Org. Lett. 7 (2005) 5039.
[45] H. Zhang, C.-B. Yang, Y.-Y. Li, Z.-R. Donga, J.-X. Gao, H. Nakamura, K. Murata, T. Ikariya, Chem. Commun. (2003) 142.
[46] E.A. Nyawade, H.B. Friedrich, B. Omondi, P. Mpungose, Organometallics 34 (2015) 4922.
[47] H.B. Friedrich, V. Gokul, J. Mol. Catal. A: Chem. 271 (2007) 277.
[48] L. Gonsalvi, I.W.C.E. Arends, P. Moilanen, R.A. Sheldon, Adv. Synth. Catal. 345 (2003) 1321.
[49] A.S. Goldstein, R.S. Drago, J .Chem. Soc., Chem. Commun. (1991) 21.
[50] K.N. Kumar, G. Venkatachalam, R. Ramesh, Y. Liu, Polyhedron 27 (2008) 157.
[51] A.M. El-Hendawy, A.H. Alkubaisi, A.E.-G. El-Kourashy, M.M. Shanab, Polyhedron 12 (1993) 2343.

Synthesis and characterization of piano-stool ruthenium complexes with N, N′-pyridine imine bidentate ligands and their application in styrene oxidation.

Research Highlights

- New arene ruthenium(II) pyridine-imine complexes have been prepared
- Their crystal structure show the pseudo-octahedral piano stool geometry
- The complexes were applied in the oxidation of olefins in a H_2O/t-butanol mixture
- IR and UV-vis studies suggest the mechanism involves a Ru(IV) oxo species